Turk J Chem
25 (2001) , 241 – 249.

Investigation of the Microporous and Mesoporous Structures of the Reşadiye (Tokat/Turkey) Bentonite and its Fractions

Müşerref ÖNAL, Yüksel SARIKAYA, Tülay ALEMDAROĞLU
University of Ankara, Faculty of Science, Department of Chemistry, Tandoğan, 06100 Ankara-TURKEY

Received 13.06.2000

It was determined by X-ray diffraction that, besides containing clay minerals such as montmorillonite and illite, the original bentonite contained also clinoptilolite, opal-C, quartz, calcite and dolomite. The original bentonite was separated into four fractions by decantation and precipitation from its aqueous suspension. The adsorption and desorption of nitrogen on the original bentonite and its fractions at 77 K were investigated. The specific surface areas of the samples were determined according to the methods of Brunauer-Emmett-Teller, de Boer-Lippens, and Harkins-Jura by using the adsorption data. The mesopore size distribution curves were plotted by using the desorption data. The specific micropore and the specific micropore-mesopore volumes were determined by the extrapolation of these curves. The correlation between the specific surface areas and the specific micropore-mesopore volumes is discussed.

Key Words: Adsorption, Bentonite, Montmorillonite, Porosity, Surface Area.

Introduction

Clays have been used since the beginning of civilization and they still keep their position among the most important industrial raw materials. Clays, which are used in more than 100 application areas, contain clay minerals, non-clay minerals and trace amounts of organic deposits[1]. If the major clay mineral in the clay is montmorillonite or a member of other smectites, then it is called bentonite. The application areas of bentonites vary depending on the kinds and amounts of its constituents such as smectites (which are the major clay minerals, other clay minerals) and non-clay minerals[2,3].

The application of bentonites in the production of selective adsorbants[4−6], bleaching earth[7,8], catalyst beds[9], carbonless copy paper[10] and medication[11], depends on the porous structures of smectites. The pores are assumed to be cylindrical. If the pore radii are smaller than 1nm, these are called micropores. If their radii are between 1 nm and 25 nm, these are called mesopores and if their radii are bigger than 25 nm, these are called macropores. The adsorption capacity of the macropores is at a negligible level when compared to that of the micropores and mesopores.

When an adsorption equilibrium is established, the adsorbed substance in one gram of the adsorbent is called the adsorption capacity. The adsorption capacity can be represented by n (mol g^{-1}) or by v^g

(cm^3 g^{-1}) which is the ideal gas volume normalized under the conditions of 273 K and 1 atm, or by v^l (cm^3 g^{-1}) which is the volume of liquid nitrogen at 77 K. The relation between the above adsorption capacities can be given as follows:

$$n/\text{mol } g^{-1} = v^g(\text{cm}^3 g^{-1})/24200\text{cm}^3\text{mol}^{-1} = v^l(\text{cm}^3 g^{-1})/34.65 cm^3\text{mol}^{-1} \quad (1)$$

where 24000 cm^3mol^{-1} is the normalized molar volume of the nitrogen gas, which is assumed to behave as an ideal gas, and 34.65 cm^3 mol^{-1} is the molar volume of liquid nitrogen at 77 K. The adsorption capacity (v^l / cm^3 g^{-1}) obtained from the desorption isotherms, which is given as the volume of liquid nitrogen, can be taken as the specific volume of the pores which are still full.

The adsorption capacity necessary for monomolecular adsorption is called the monolayer capacity. The monolayer capacity can be represented as n_m (mol g^{-1}), as v_m^g(cm^3 g^{-1}) or as v_m^l(cm^3 g^{-1}). The total area occupied by the molecules within the monolayer capacity is defined as the specific surface area[12]. The specific surface area (A) can be calculated from the following equation[13] by using only the nitrogen adsorption data.

$$A/m^2g^{-1} = 97524(n_m/\text{mol } g^{-1}) \quad (2)$$

There are large bentonite reserves in different regions of Turkey. In order to use these bentonites more efficiently, their porous structures need to be investigated in addition to their other properties. Therefore, the aim of this study was to determine the microporous and mesoporous structures of the Reşadiye (Tokat/Turkey) bentonite and its fractions by nitrogen adsorption at 77 K.

Materials and Methods

The Reşadiye (Tokat/Turkey) bentonite was used as the material of this study. The natural bentonite was ground to pass through a 0.074 mm sieve. It was dried for four hours at 105°C. A 20 g specimen was taken from the dried bentonite (R0), 1000 g of distilled water was added and the mixture was stirred for 15 minutes with a magnetic stirrer. The suspension thus prepared was then left to rest. The fraction which precipitated in 15 minutes from the suspension was labeled R1. The fraction which precipitated in 3 days from R1 was labeled R2, the fraction which precipitated in one week (considered as infinite time) from R2 was labeled R3, and the fraction which stayed continuously in suspension was labeled R4. The chemical analysis of the R3 and R4 fractions was performed and their equivalent Na^+/Ca^{2+} ratios were determined.

The XRD patterns of R0, R4, R4 heated for 1 hour at 550°C and R4 swollen with ethylene glycol were determined respectively. The XRD analysis was performed with a Philips PW 1730 powder diffractometer, using CuKα X-rays whose wavelength was 1.5418 nm, and a Ni filter was used.

The isotherms of the adsorption and desorption of nitrogen at 77 K on the R0, R1, R2, R3 and R4 samples were determined. A volumetric adsorption instrument, under vacuum, fully constructed of Pyrex glass was used in the experiments[14].

Results and Discussion

It was determined that R0 contained 25% R1, 18% R2, 7% R3, and 50% R4, represented in mass percents. It is well known that CaM precipitates from the aqueous suspension whereas NaM does not precipitate at all.

Therefore it was judged that the R3 fraction was Ca-rich montmorillonite (CaM) and the R4 fraction was Na-rich montmorillonite (NaM). The fact that the equivalent Na^+/Ca^{2+} ratios in the R3 and R4 fractions were respectively determined as 0.20 and 0.75, verified this judgement.

The XRD patterns of R0, R0 heated for 1 h at 550°C, R4, and R4 swollen in ethylene glycol are given in Figure 1. From the XRD patterns of R0, it was observed that the major clay mineral in the original bentonite was NaM, and the second clay mineral was illite. The non-clay minerals present in the original bentonite were clinoptilolite, opal-C, quartz, calcite and dolomite[15].

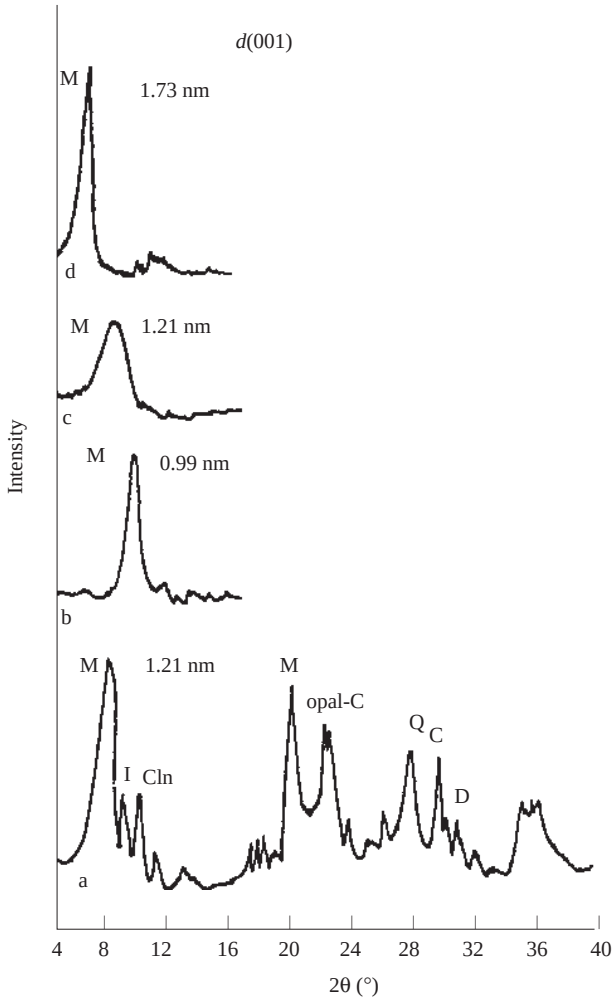

Figure 1. The XRD patterns of the original Reşadiye bentonite (R0), R0 heated at 550°C for 1h, purified NaM (R4), and R4 swollen in ethylene glycol (M: montmorillonite, I: illite, Cln: clinoptilolite, Q: quartz, C: calcite, D: dolomite).

When the R4 fraction was swollen by ethylene glycol, its $d(001)$ value increased from 1.21 nm to 1.73 nm. When the R4 fraction was heated for 1 h at approximately 550°C, its $d(001)$ value decreased from 1.21 nm to 0.99 nm because of the elimination of the monomolecular water layer between the NaM layers. As a result, the nonaqueous TOT layer thickness could be taken as 0.99 nm.

The isotherms of the adsorption of nitrogen on the R0, R1, R2, R3 and R4 samples, at 77 K, are given in Figure 2. Here, p^o is the adsorption equilibrium pressure, p^o is the condensation pressure of nitrogen and

$p/p^0 \equiv x$ is the relative equilibrium pressure. It was observed that the adsorption capacity increased in the order $R1 < R0 \approx R2 < R4 < R3$.

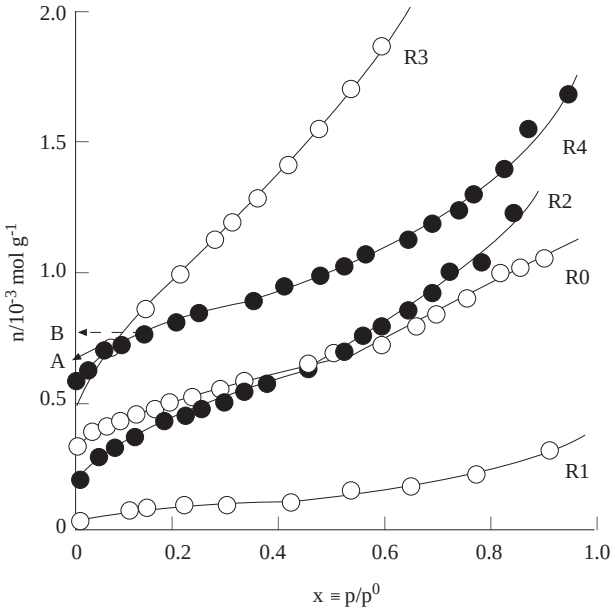

Figure 2. The isotherms of the adsorption of nitrogen on the original bentonite and its fractions.

The A and B points were found by the extrapolation of the linear parts of the adsorption isotherms at $x = 0$, and they are marked on the adsorption isotherm of R4 in Figure 1. The specific surface areas of each sample were calculated from the monolayer capacities, which were determined according to the A and B methods[13].

The adsorption isotherm equations, which were derived by Brunauer-Emmett-Teller (BET)[12,13,16], de Boer-Lippens (BL)[12,17,18] and Harkins-Jura (HJ)[12,13,19] can be expressed in the form of straight line equations as follows:

$$x/n(1-x) = 1/n_m c + [(c-1)/n_m c]x \tag{3}$$

$$v^l/\mathrm{cm}^3 g^{-1} = A(m^2 g^{-1})(t/nm)/997; \quad t/nm = 0.73/[\ln(1/x)]^{1/3} \tag{4}$$

$$\ln x = B - C/(v^g/\mathrm{cm}^3 g^{-1}); \quad A/m^2 g^{-1} = 4.06 C^{1/2} \ (\mathrm{for} N_2) \tag{5}$$

where c, B and C represent constants related to temperature, adsorbent and adsorbed respectively, and t represents the thickness of the adsorption layer. To see whether the adsorption data satisfied the BET, BL and HJ equations or not, the graphs in Figures 3, 4 and 5 were plotted. The straight lines seen in these graphs verify that the adsorption data satisfy all of the isotherm equations: The A values were calculated as follows; i) The n_m values, which were calculated by the simultaneous solution of the equations obtained from the slopes and the intercepts on the vertical axis of the BET straight lines, were substituted in Equation 1 and the A values were calculated; ii) The A values were directly calculated from the slopes of the BL straight lines; iii) The C values which were equal to the slopes of the straight lines seen in Figure 5 were substituted in Equation 5 and the HJ specific surface areas were determined.

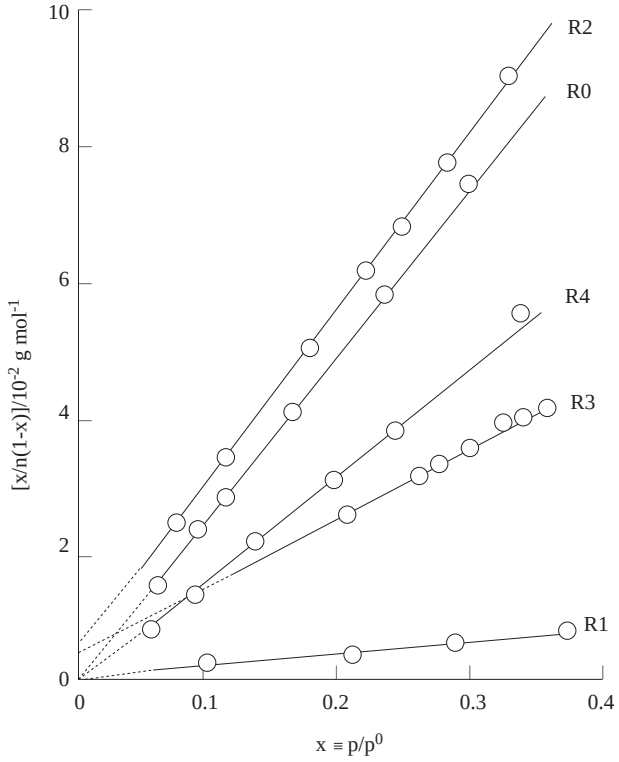

Figure 3. The Brunauer-Emmett-Teller (BET) straight lines of the investigated samples.

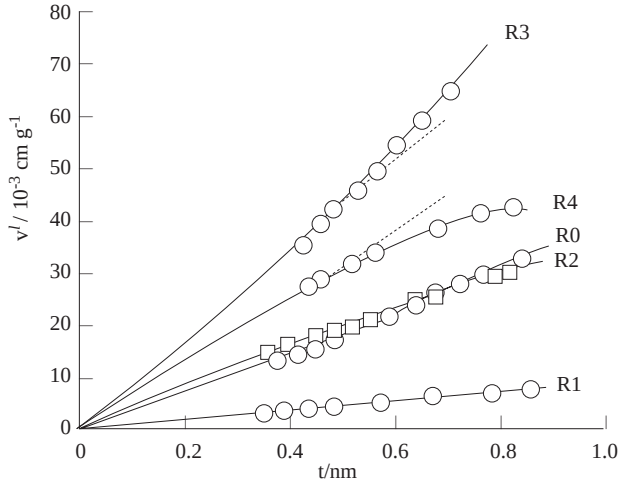

Figure 4. The de Boer-Lippens (BL) $v^l - t$ graphs of the investigated samples.

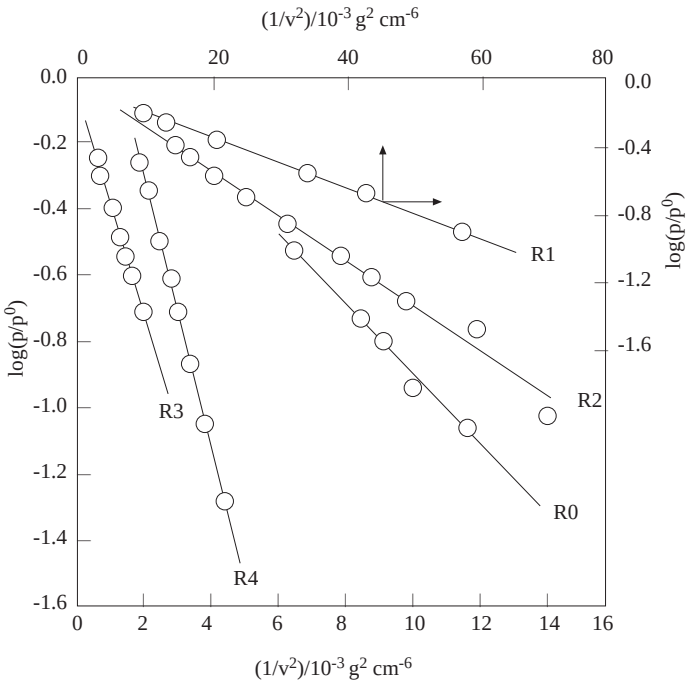

Figure 5. The Harkins-Jura (HJ) straight lines of the investigated samples.

The correlation between the specific surface areas which were calculated according to different pro-

cedures and the correlation between those and and the specific surface areas calculated according to the standard BET method are given in Figure 6. It was observed that there was a good correlation between the surface areas calculated according to the BET method and those calculated according to the BL equations. Since the BET and BL isotherm equations had been deriven for multimolecular adsorption, this good correlation showed that the adsorption was multimolecular. The deviation of the A, B and HJ specific surface areas from those of the BET and from each other increased, as the specific surface area increased. On the other hand, there was a better correlation between the specific surface areas calculated according to the A and B methods.

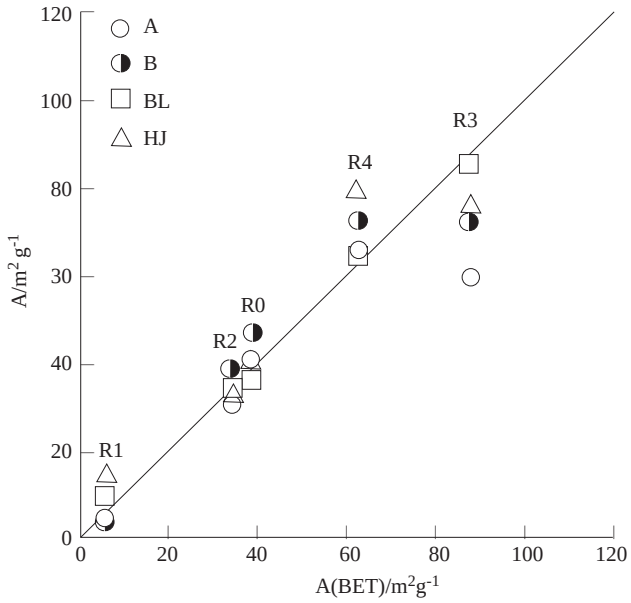

Figure 6. The correlation between the specific surface areas determined by the other methods and the specific surface areas determined by the BET method.

The corrected Kelvin equation which relates the radii of the mesopores to the desorption equilibrium pressure takes the form given below[13]

$$r/nm = 0.952/\ln x + 0.735/(\ln x)^{1/3} \tag{6}$$

By using Equations 1 and 6 the $v^l_{mm} - r$ mesopore size distribution curves were plotted from the desorption data. These curves are shown in Figure 7 for each sample. It was observed that the porosity of the investigated samples increased in the order$R1 < R0 \leq R2 < R4 < R3$. It was understood that the original bentonite and the fractions, except R1, could be used as adsorbents. It can be stated that R2, which has a higher porosity than R0, contains a considerable amount of CaM. On the other hand, it was verified that the R4 sample, which contained mainly mesopores of smaller radii, was pure NaM, and the R3 sample, which contained mainly mesopores of larger radii, was a mixture of CaM and opal-C. For each sample, the v^l_{mi} and v^l_{mm} specific pore volumes were determined by the extrapolation of the $v^l - r$ curves at $r = 1\ nm$ and $r = 25\ nm$, and the v^l_{me} sspecific mesopore volumes were determined from the difference between the specific pore volumes.

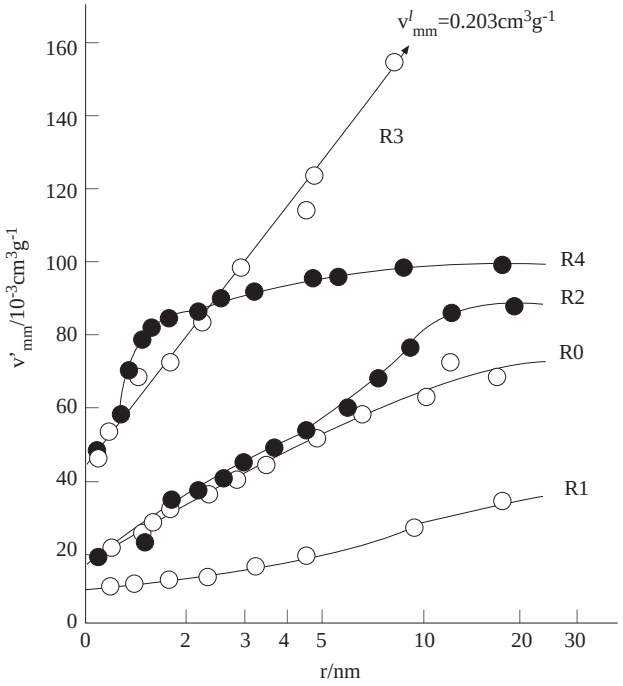

Figure 7. The $v^l_{mm} - r$ mesopore size distribution curves of the investigated samples.

The variation in the BET specific surface areas as a function of the specific micropore-mesopore volumes is given in Figure 8. The increase in the A(BET) values was first sharp as the v^l_{mm} values increased, but then it became mild. The reason for this behaviour was that as the pore radius of the mesopores increased the specific pore volume increased continuously but the specific surface area did not increase to the same extent, since the number of walls which separate the pores decreased.

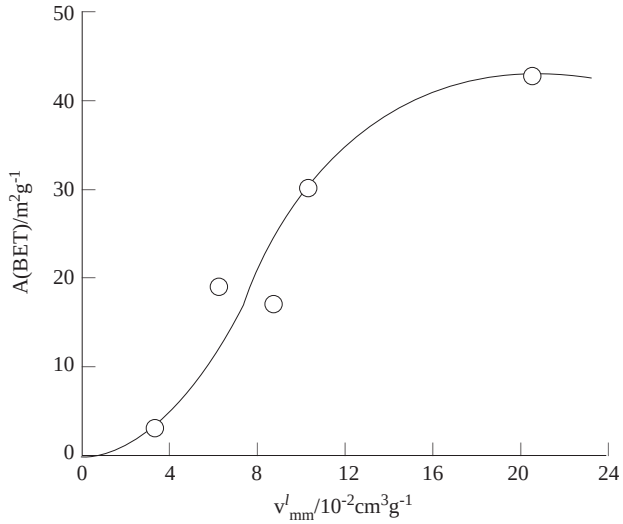

Figure 8. The relationship between the specific surface areas determined by the BET method and the specific micropore-mesopore volumes.

It is assumed that the micropore volumes are filled at the end of monomolecular adsorption[20]. Therefore, the monomolecular adsorption capacity (v^l_m) can be taken as equal to the specific micropore

volume (v^l_{mi})[21]. The adsorption isotherm equation according to the volume filling theory developed by Polonyi-Dubinin-Raduskevich-Kaganer (PDRK) is given as follows[13,20,21]:

$$\ln v^l = \ln v^l_{mi} - D[\ln(p^0/p)]^2 \tag{7}$$

Here, D represents a constant which is a function of the adsorbent, the adsorbed and temperature. The graphs $\ln\, v^l - [\ln(p^0/p)]^2$, plotted by using the adsorption isotherms, are given in Figure 9. Straight lines which satisfy Equation 7 were obtained by joining the points corresponding to low p/p^0 i.e., high p^0/p values at which the monomolecular adsorption is completed. The v^l_{mi} values were obtained from the intercepts on the vertical axis of these straight lines.

The relationship between the specific micropore volumes calculated by two different methods is given in Figure 10. It was clear that although the v^l_{mi} values which were determined by the extrapolation of the $v^l - r$ curves at $r = 1\ nm$ were bigger than the v^l_{mi} (PDRK) values, there was an almost linear relationship between them.

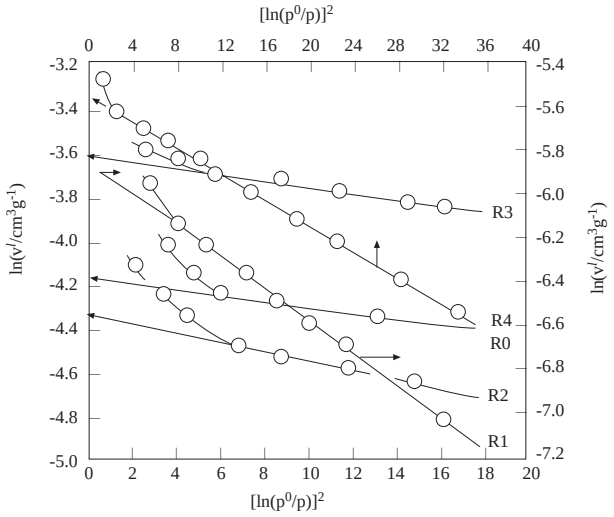

Figure 9. The Polonyi-Dubinin-Raduskevich-Kaganer (PDRK) graphs of the investigated samples.

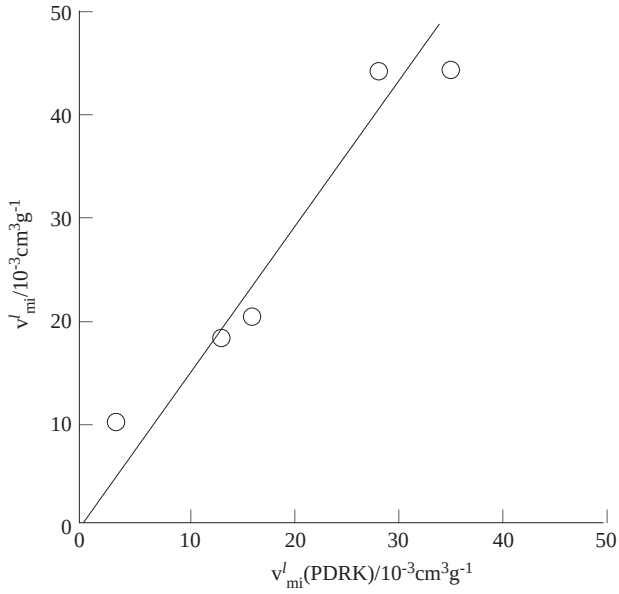

Figure 10. The correlation between specific micropore volumes found respectively from the $v^l_{mm} - r$ and PDRK graphs.

Conclusion

It was determined that Na-rich montmorillonite and Ca-rich montmorillonite could be obtained from the Reşadiye bentonite by precipitation and decantation of its aqueous suspension. It was observed that the specific surface areas which were calculated according to the BET and BL methods from the adsorption data were in good correlation. It appeared that NaM and CaM were typical mesoporous adsorbents. It was concluded that the original bentonite and its fractions (except the R0 faction which precipitated in the first 15 min from the aqueous suspension) was suitable for use as an adsorbent for the adsorptions the gas phase, vapour phase and also the discharge waters and solutions.

Acknowledgments

The authors thank the Ankara University Research Fund for funding this work by the project 96-05-04-02. The authors are also grateful to Eczacıbaşı Ceramic Industries for their help in the experimental studies.

References

1. H. H. Murray, **Appl. Clay Sci. 5**, 379-95 (1991).
2. R. E. Grim and N. Güven, **Bentonites - Geology, Mineralogy, Properties and Uses, (Developments in Sedimentology, 24),** Elsevier, New York, 1978.
3. R. E. Grim, **Clay Mineralogy**, 2^{nd} ed., McGraw-Hill, New York, 1968.
4. R. M. Barrer, **Zeolites and Clay Minerals as Sorbents and Molecular Sieves,** Academic Press, London, 1978.
5. R. M. Barrer, Clay. **Clay Miner. 37**, 385-95 (1989).
6. R. M. Barrer, **Pure Appl. Chem. 61**,1903-12 (1989).
7. M. K. H. Sıddıquie, **Bleaching Earth,** Pergamon Press, London, 1968.
8. E. Srasra, F. Bergaya, H. van Damme and N. K. Ariquib, **Appl. Clay Sci. 4,** 411-21 (1989).
9. T. J. Pinnavia,**Science 220**, 365-71 (1983).
10. M. Takasima, S. Sano and S. Ohara, **J. Imaging Sci. Techn. 37,** 163-66 (1993).
11. E. Gomiz, J. Linares and R. Delgado, **Appl. Clay Sci. 6,** 359-68 (1992).
12. H. Ceylan and Y. Sarıkaya, **Doğa, TU Kim. D. C. 12,** 147-56 (1988).
13. S. J. Gregg and K. S. W. Sing, **Adsorption, Surface Area and Porosity,** 2^{nd} ed., Academic Press, London, 1982.
14. Y. Sarıkaya and S. Aybar, **Commun. Fac. Sci. Uni. Ank. B24,** 33-9 (1978).
15. G. W. Brindley and G. Brown, **Crystal Structure of Clay Minerals and Their X-Ray Identification,** Mineralogical Soc., London, 1980.
16. S. Brunauer, P. H. Emmett and E. Teller, **J. Am. Chem. Soc. 60,** 309-19 (1938).
17. B. G. Linsen (ed.), **Physical and Chemical Aspects of Adsorbents and Catalysts,** Academic Press, London, 1970.
18. B. C. Lippens and J. H. de Boer, **J. Catal. 4**, 319-23 (1965).
19. W. D. Harkins and G. Jura, **J. Am. Chem. Soc. 66,** 1366-73 (1944).
20. M. G. Kaganer, **Dokl. Akad. Nauk. SSR, 138,** 419-22 (1961).
21. M. M. Dubinin, **J. Colloid Interf. Sci. 23,** 487-99 (1967).